Weak stochastic ratchets and dynamic localization in measurement-induced quantum trajectories

I. Babushkin
Institute of Quantum Optics, Leibniz University Hannover, Welfengarten 1, 30167 Hannover, Germany
and Max Born Institute, Max-Born-Strasse 2a, 10117 Berlin, Germany
(Received 9 June 2016; published 3 April 2017)

We consider a qubit governed by a sequence of weak measurements, with the measurement strength modified in a time- and state-dependent manner. Here we show that the resulting trajectory of the qubit in the phase space can be weakly controlled without any direct action on the qubit (control-free control), even if only one fixed observable is measured. In particular, we demonstrate a possibility of a weak form of a stochastic ratchet, allowing us to weakly push the qubit's state without any net force in the effective potential. Furthermore, if the weak measurement strength is significantly reduced in a way conditioned to some particular state, a dynamical localization near this state takes place. If the measurement strength is reduced to zero, a singularity appears, which behaves like an artificial basis state.

DOI: 10.1103/PhysRevA.95.042101

I. INTRODUCTION

Dynamics of quantum systems with the states frequently monitored by a measurement apparatus can be rather controversial and is a subject of constant interest over the years [1–15]. Every measurement in the measurement sequence may be tuned to cause only a partial collapse of the system's wave function, with the collapse effect being arbitrarily weak (so-called "weak measurements") [4,8,16–18]. In another context, the term "weak measurement" was introduced by Aharonov, Albert, and Vaidman (AAV) [19] as being attributed to a measurement of a continuous degree of freedom (e.g., an electron position) coupled to a discrete one (spin) via postselection. These two approaches were recently shown to be equivalent [20,21]. As a result of repetitive application of weak measurements—the situation which is sometimes referred to as weak Zeno measurements (WZMs)—a kind of stochastic "quantum trajectory" arises [3,14,22–24] due to unpredictable character of every particular measurement outcome.

Just repeating the weak measurements, without any further action on the system, allows us to control the system state in various ways. For instance, one can achieve an arbitrary state from any other one by repeating weak measurements in different bases [2,5,6,12,13,25,26]. Alternatively, by allowing the strength of the weak measurements (in the AAV sense) to depend on the spatial coordinate, one can create a "potential wall" which may reflect a particle [12,13]. It should be noted that these control mechanisms work if the initial state is preknown.

In contrast, if we repeat a weak measurement of a single qubit in a fixed basis, the resulting dynamics was up to now believed to be very trivial. The resulting quantum trajectory just stochastically approaches one of the two qubit's basis states $|0\rangle$ or $|1\rangle$. In this article we add an another dimension to this seemingly trivial dynamics by allowing the measurement strength to be changed in time and in a state-conditional way.

We observe that the stochastic equations, describing quantum trajectories in such a simple one-dimensional system, are in fact quite similar to the ones describing motion of a small Brownian particle in a fluid flow (overdamped Brownian motion) [23,27–29]. One of the striking phenomena in such flows as well as in many other stochastic systems are so-called stochastic ratchets [27–50]. Namely, by varying the potential acting on the Brownian particle in time and/or space in a periodic way, it is possible to create an effective additional force, despite that the potential introduces no average force. Brownian ratchets are deeply connected to so-called Parrondo games, when two or more lossy games are combined to give a winning one [30,36–48]. Very recently, the notion of weak Parrondo games and weak Brownian ratchets were introduced in [30] to describe the situation when two or more lossy games are played together to give a just less lossy (but not winning) one. We remark that, although both Parrondo games and Brownian ratchets were considered in the context of quantum systems [28,38–41], this was up to now done via some direct action on the system itself.

In contrast, in the present article the situation of control-without-direct-action will be discussed. Here we show how the effective potential arising in WZM dynamics can be modified by changing the strength of the measurement periodically in time and in a state-conditioned fashion (that is, in dependence on the current system state). We demonstrate that the stochastic ratchet effect, albeit weak, is possible in such a situation. We also demonstrate a dynamic localization of the state in the case when the measurement strength vanishes at some particular system state. A "false basis state" may appear, which "attracts" the stochastic trajectories in a similar way as the true basis states do.

The article is organized as follows: In Sec. II we introduce the system under consideration and derive the master equation governing the probability distribution on the line between two basis states. In Sec. III we derive the equation for the continuous case taking into account conditionally dependent measurement strength. In Secs. IV and V we investigate the effects related to the conditionally modified measurements strength. Finally, the conclusions and discussion are presented in Sec. VI.

II. DISCRETE DYNAMICS

A. Setting

Our model of weak Zeno measurements is depicted in Fig. 1(a) and uses projective measurements of ancilla qubit $|a\rangle$ to realize the weak ones of $|q\rangle$. The system is prepared in the state $|q\rangle \otimes |0\rangle$ with $|q\rangle = \cos\theta|0\rangle + \sin\theta|1\rangle$ for some

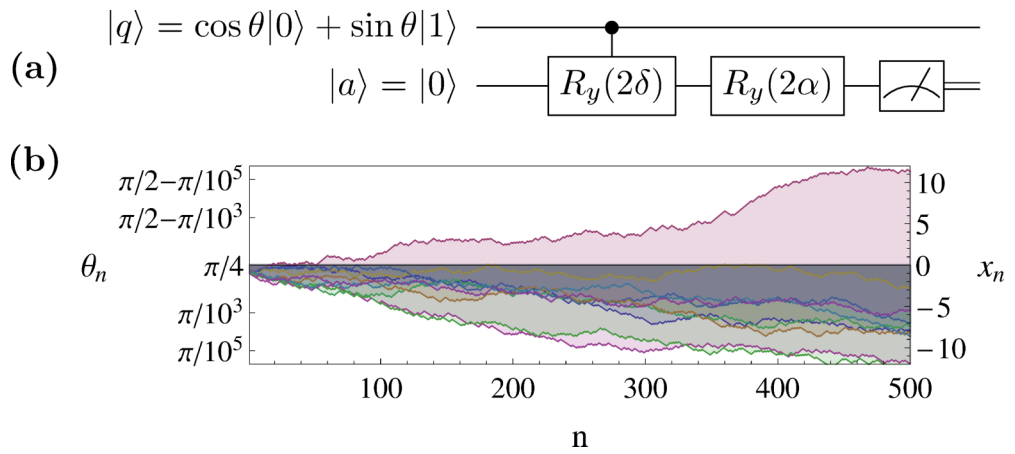

FIG. 1. (a) The model of weak measurements of the qubit $|q\rangle$ using an ancilla $|a\rangle$ (initially in the state $|0\rangle$) and its rotations R_y, followed by the measurement of $|a\rangle$. After the measurement, the process is repeated with the same or another ancilla in the state $|0\rangle$. In (b), several exemplary stochastic trajectories induced by repeating application of (a) using θ coordinate (left y axis) and x coordinate given by Eq. (10) (right y axis) vs measurement number n are shown. The x coordinates are obviously better suited to study the asymptotic behavior as $n \to \infty$.

θ. First, we apply a rotation $R_y(2\delta)$ to the ancilla state; the rotation R_y is conditioned to $|q\rangle = |1\rangle$ and is defined as

$$R_y(\delta)|0\rangle \mapsto \cos\delta|0\rangle + \sin\delta|1\rangle, \tag{1}$$

$$R_y(\delta)|1\rangle \mapsto \cos\delta|1\rangle - \sin\delta|0\rangle. \tag{2}$$

Afterwards, we unconditionally apply the rotation R_y by some angle α and finally measure the ancilla qubit. If $\alpha \neq 0$ and δ is small, the resulting measurement modifies $|q\rangle$ only slightly. After the measurement, we repeat the whole procedure using another ancilla in the initial state $|0\rangle$ (or the same ancilla returned to the state $|0\rangle$).

The state of the whole system $|q\rangle \otimes |0\rangle$ [see Fig. 1(a)] is transformed by two R_y operators described above as

$$|q\rangle \otimes |0\rangle \mapsto |q_0\rangle \otimes |0\rangle + |q_1\rangle \otimes |1\rangle, \tag{3}$$

$$|q_i\rangle = \sum_j b_{ij}|j\rangle, \tag{4}$$

where b_{ij} are the $(i+1, j+1)$th element of the matrix b defined as

$$b = \begin{pmatrix} \cos\theta\cos\alpha & \sin\theta\cos(\delta+\alpha) \\ \cos\theta\sin\alpha & \sin\theta\sin(\delta+\alpha) \end{pmatrix}. \tag{5}$$

If the measurement of $|a\rangle$ gives 0, the system state is reduced to $|q\rangle = |q_0\rangle/\sqrt{p_0}$ and in the opposite case to $|q\rangle = |q_1\rangle/\sqrt{p_1}$, where

$$p_0 = \cos^2\alpha\cos^2\theta + \sin^2\theta\cos^2(\delta+\alpha), \tag{6}$$

$$p_1 = \cos^2\theta\sin^2\alpha + \sin^2\theta\sin^2(\delta+\alpha). \tag{7}$$

The probabilities of the corresponding outcomes are p_0 and p_1.

The above description can be reformulated in the form of a generalized measurement formalism, with the measurement operators

$$\mathcal{B}_0 = b_{11}|0\rangle\langle 0| + b_{12}|1\rangle\langle 1|, \tag{8}$$

$$\mathcal{B}_1 = b_{21}|0\rangle\langle 0| + b_{22}|1\rangle\langle 1|, \tag{9}$$

so that $\sum_j \mathcal{B}_j^\dagger \mathcal{B}_j = 1$ and the state after the measurement with the result j is transformed as $|q\rangle \to \mathcal{B}_j|q\rangle/\sqrt{p_j}$.

The resulting process is a (classical) one-dimensional random walk along the axis θ as shown in Fig. 1(b). It spends most of the time in the vicinity of the limiting states $|q\rangle = |0\rangle$ and $|q\rangle = |1\rangle$ ($\theta = 0,\ \pi/2$). It is thus useful to introduce parabolic coordinates [17] as

$$x = \operatorname{atanh}\{-\cos(2\theta)\}; \quad \theta = \arcsin\sqrt{\frac{1+\tanh x}{2}}. \tag{10}$$

In this coordinate system, $\theta = 0$ corresponds to $x = -\infty$ and $\theta = \pi/2$ corresponds to $x = +\infty$ [(cf. Fig. 1(b)]. Using x instead of θ allows us to expand these vicinities into semi-infinite intervals. We also note that if we measure $|q\rangle$ directly (instead of $|a\rangle$), the probability to find $|q\rangle$ in the state $|1\rangle$ will be

$$\Pi(x) = \sin^2\theta = (1+\tanh x)/2. \tag{11}$$

B. Classical random-walk interpretation

Now, for the sake of simplicity, we exclude the situation when $|q\rangle$ is exactly in one of the basis states $|0\rangle$ or $|1\rangle$ in the beginning of the process. In this case, the equations above allow us to define the process as a one-dimensional random walk on the line $x \in (-\infty, +\infty)$ in the following way: assuming that at the nth iteration step the system is in the point x_n, at the $n+1$ step it will be in the point either $x_{n+1} = x_n + \epsilon_0$ or $x_{n+1} = x_n + \epsilon_1$ (depending on the measurement outcome), every of two variants occurring with the probabilities $p_i(x_n)$, $i = 0,1$. A few realizations of this random walk are shown in Fig. 1(b).

The probabilities $p_i(x)$ can be rewritten in x coordinates as

$$p_0(x) = \Pi(x)\cos^2(\delta+\alpha) + [1-\Pi(x)]\cos^2\alpha, \tag{12}$$

$$p_1(x) = \Pi(x)\sin^2(\delta+\alpha) + [1-\Pi(x)]\sin^2\alpha, \tag{13}$$

where $\Pi(x)$ is defined by Eq. (11). The step sizes ϵ_i, $i = 0,1$, do not depend on x and are given by (see details

in Appendix A)

$$\epsilon_0 = \operatorname{atanh}\left(\frac{2\cos^2(\alpha+\delta)}{\cos^2(\delta+\alpha)+\cos^2\alpha} - 1\right), \tag{14}$$

$$\epsilon_1 = \operatorname{atanh}\left(\frac{2\sin^2(\alpha+\delta)}{\sin^2(\delta+\alpha)+\sin^2\alpha} - 1\right). \tag{15}$$

Equations (12)–(15) define obviously a Markovian random walk.

C. Conditionally varied measurement parameters

Suppose we know exactly the initial state of the system x_0 and are able to make all the rotations also exactly. In this case, the subsequent positions x_n of the qubit on x line can be also calculated exactly since we know the measurement outcomes $M_n = 0,1$ and thus the step sizes ϵ_i at every n. We may now introduce the state-dependent dynamics by allowing the parameters δ, α to be dependent on the step number n and the state of the system at the last step x_n. That is, we may take some (predefined) functions of two arguments $\alpha(n,x)$, $\delta(n,x)$ and at every step select the parameters for the next step α_{n+1}, δ_{n+1} as $\alpha_{n+1} = \alpha(n,x_n)$, $\delta_{n+1} = \delta(n,x_n)$. In this way, the parameters p_i, ϵ_i of our random walk will be also some predefined functions of n, x_n [defined by Eqs. (12)–(15)].

The functions $\alpha(m,x)$, $\delta(m,x)$ may be quite arbitrary. They add new degrees of freedom to our system, leading, as we will see, to rather interesting dynamics. We remark also that in quantum control schemes [14] the information about the current state of the system is often used by feeding it back into the system via modification of the system's Hamiltonian. In contrast, in our case, only the parameters of the measurement itself, but not the parameters of the system, are changed.

D. Master equation

Using Eqs. (3)–(5) or Eqs. (8) and (9) it is easy to obtain an equation governing the evolution of the probability density function (pdf) $P(n,x)$, describing the probability P of $|q\rangle$ to appear in the vicinity of x at the step n. Since our qubit $|q\rangle$ always remains in a pure state which is fully described by its coordinate x (or, equivalently, by θ), such a master equation is just another way to express the dynamics of $|q\rangle$. It provides essentially the same information as Eqs. (3)–(5). This reformulation will, however, be useful in the next sections when we consider stochastic ratchet behavior.

We start from the general case with no assumption about the particular coordinate system. We use the variable y by which we may understand any of the coordinates x, θ, or Π mentioned before. We introduce furthermore the measure $d\mathcal{P}(n,y) = P(n,y)dy$ which expresses the total probability to find $|q\rangle$ in the interval $[y, y+dy]$. Then, by definition of our process, using the Markov property and the formula for total probability [42] we obtain the following relation:

$$\begin{aligned} d\mathcal{P}(n+1,y) = {} & p_0(y_0(y))d\mathcal{P}(n,y_0(y)) \\ & + p_1(y_1(y))d\mathcal{P}(n,y_1(y)), \end{aligned} \tag{16}$$

where $y_i(y)$, $i = 1,2$ are defined in an implicit way as $y = y_i + \epsilon_i(y_i)$. This expression is valid for an arbitrary (also varying) step size, that is, also for the state-conditioned trajectories as they were defined above in the previous section. In the case of x coordinates ($y \equiv x$) we obtain straightforwardly the following expression for $P(n,x)$:

$$\begin{aligned} P(n+1,y) = {} & p_0(x_0(x))x_0'(x)P(n,x_0(x)) \\ & + p_1(x_1(x))x_1'(x)P(n,x_1(x)), \end{aligned} \tag{17}$$

where $x = x_i(x) + \epsilon_i(x_i(x))$, $x_i'(x) = dx_i(x)/dx$. In particular, for the constant measurement strength we have $\epsilon_i = \text{const}$, $x_i'(x) = 0$, and therefore

$$\begin{aligned} P(n+1,x) = {} & p_0(x-\epsilon_0)P(n,x-\epsilon_0) \\ & + p_1(x-\epsilon_1)P(n,x-\epsilon_1). \end{aligned} \tag{18}$$

Very important are conserved quantities of Eq. (16) or Eq. (17). The most obvious one is the average value of Π on nth step, $\langle\Pi\rangle_n \equiv \int_{-\infty}^{+\infty}\Pi(x)P(n,x)dx$, which represents the *a priori* probability to find $|q\rangle$ in the state $|1\rangle$ if we perform a projective measurement of $|q\rangle$ after the nth step of our process. One can show that from Eq. (18) it follows that

$$\langle\Pi\rangle_{n+1} = \langle\Pi\rangle_n, \tag{19}$$

and thus for any n, $\langle\Pi\rangle_n = \langle\Pi\rangle_0$. Equation (19) can be obtained by substituting Eq. (17) into the definition of $\langle\Pi\rangle_{n+1}$, giving thus

$$\begin{aligned} \langle\Pi\rangle_{n+1} &= \int_{-\infty}^{+\infty}\Pi(x)P(n+1,x)dx \\ &= \int_{-\infty}^{+\infty}P(n,x)\{p_0(x)\Pi(x) + p_1(x)\Pi(x)\}dx, \end{aligned} \tag{20}$$

where we made a replacement $x_i'(x)dx \to dx_i$ and the variable change $x_i(x) \to x$ in both parts of the resulting integral. Since $p_0(x) + p_1(x) = 1$, this gives Eq. (19). We remark that Eq. (19) is universal, that is, valid for any choice of the measurement parameters, also if they vary in dependence on the step n or current position x_n.

III. CONTINUOUS DIFFUSIVE LIMIT

A. General equation

The continuous limit arises if we tend the measurement strength to zero. In this case, instead of the discrete equation (17), a continuous equation arises, with the step numbers n being mapped to a continuous "time" t. If the measurement strength is constant (independent on n) and if this constant strength tends to zero, the corresponding limit is universal, that is, does not depend on the measurement strength and on the particular measurement procedure. The dynamics in such an "unconditional" continuous limit is often described by the stochastic Schrödinger equation or by the master equation for the density matrix [14,17,18,22–24,43]. Nevertheless, to our knowledge, a consideration general enough to include time- and conditionally varied measurements were presented only very recently in [44]. Earlier works dealt only with the case of measurements of equal strength or at least the strength which is not explicitly time dependent (but might depend on time indirectly via the outcome of the previous measurement) [17,18]. Instead of directly writing the resulting equation according to [44] we will proceed, for the sake of closeness of presentation, from the master equation for

$P(n,x)$, derived in the previous section, to the corresponding continuous limit described by the so called Fokker-Planck (FP) equation [28,42]. The FP approach used here is also different from [44] where Ito calculus is used, but Ito and FP approaches are, of course, equivalent [42]. We use the latter because of the straightforward connection to the methods used in the theory of stochastic ratchets [28].

That is, our goal here is to derive the FP equation in the case which includes the walk with conditionally varying measurement parameters δ, α which depend on the outcome of all the previous measurements and also on n. The transition to the continuous time can be done as follows: We introduce "time" t such that each step of our process corresponds to a small interval $\tau_n = \tau(\delta_n(n,x_{n-1}),\alpha_n(n,x_{n-1}))$, that is, we replace $n = \sum_{i=1}^{n} 1$ by

$$t \equiv \sum_{i=1}^{n} \tau_i \tag{21}$$

and allow $\tau_i(x_i)$ to tend to zero for every i, x_i. We do not assume that all τ_i are equal. In our case, as $\tau_i(x_i) \to 0$, we can expect that $P(t,x) \equiv P(n,x)|_{n\to t}$ changes at every step only slightly and we can then decompose $P(t,x)$ into series as

$$P(t+\tau_n,x) \approxeq P(t,x) + \tau_n \partial_t P(t,x). \tag{22}$$

To be allowed to do this we must assume that, independently on n, the step size $\epsilon_{i,n} = \epsilon_i(\delta_n(n,x_{n-1}),\alpha_n(n,x_{n-1}))$ defined in Eqs. (14) and (15) goes to zero as $\tau_n \to 0$. In particular, this is the case if $\delta_n \to 0$, $\alpha_n = \text{const} > 0$ for all n. Thus, for small enough δ_n, we may assume

$$\alpha_n = \text{const}(n,x), \tag{23}$$

$$\delta_n = \delta g_\delta(x_{n-1},n), \tag{24}$$

$$\tau_n = \delta^2 g_\tau(x_{n-1},n), \tag{25}$$

where we introduced the parameter $\delta \to 0$ which describes how fast δ_n and τ_n approach zero; $g_\tau(x,n) > 0$, $g_\delta(x,n)$ are some functions which do not depend on δ and which we can choose at will.

That is, we require that all τ_n, δ_n tend to zero as $O(\delta^2)$ and $O(\delta)$ respectively. This template is taken from consideration of the case with the constant step size as shown in Appendix B. The functions $g_\tau(x,n) > 0$ and $g_\delta(x,n)$ provide "form factors", which determine the strength of measurement in dependence on the system position x and n. Using Eqs. (21), (24), and (25), we define a function $g(x,t)$ as

$$g(x,t) = \left.\frac{g_\delta(x_{n-1},n)}{g_\tau(x_{n-1},n)}\right|_{n\to t;\, x_{n-1}\to x}. \tag{26}$$

Using Eqs. (22) and (26) we derive, in a rather standard way, the FP equation (see Appendix C for details and a description of the general procedure in [42]):

$$\partial_t P(t,x) = -\partial_x J(t,x), \tag{27}$$

$$J(x,y) = \mu(t,x)P(t,x) - \partial_x(D(t,x)P(t,x)). \tag{28}$$

Here

$$\mu(x,t) = g(x,t)^2 \tanh(x), \quad D(x,t) = g(x,t)^2/2 \tag{29}$$

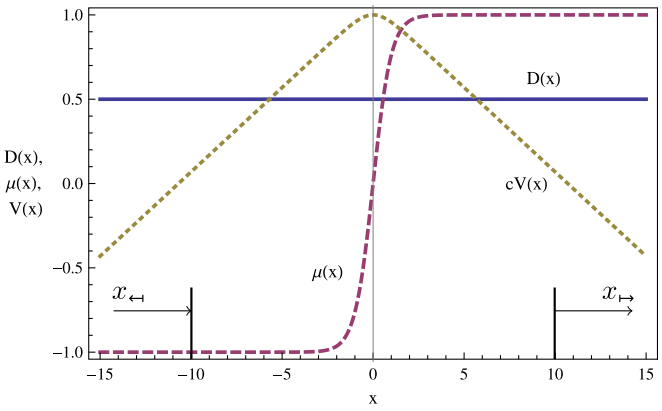

FIG. 2. Diffusion $D(x)$ (solid blue line), drift coefficient $\mu(x)$ (dashed red line) and the effective potential $V(x)$ (dotted yellow line), normalized to a constant $c = 0.1$ for better visibility in dependence on x according to Eq. (32). The asymptotic coordinates $x_{\leftarrow}$, $x_{\mapsto}$ defined in Eqs. (34) and (35) are shown, with $X = -10$ in this case. Asymptotic coordinates are useful when $|x|$ is large, that is, as $n\to\infty$: $D(x)$, $\mu(x)$, and $V(x)$ are significantly simplified in this case.

have now the meaning of the drift and diffusion coefficients, respectively. In different coordinates, like θ or Π the FP equation conserves its form; only the drift and diffusion coefficient are modified (see Appendix D).

This FP equation, as said, describes the dynamics of the pure state $|q\rangle$ whose position on the line between $|0\rangle$ and $|1\rangle$ is described by the coordinate x. Stochastic distribution of the position x is due to the unpredictable character of the weak measurement sequence. The same FP equation describes also, for instance, a Brownian heavily damped particle moving in the potential

$$V(x,t) = -\int_0^x \mu(x',t)dx' \tag{30}$$

[28,45]. The average drift velocity $\langle \dot{x}(t)\rangle \equiv \int_{-\infty}^{+\infty} \frac{dx}{dt} P(x,t)dx$ can be obtained also as an average of $J(x,t)$:

$$\langle \dot{x}(t)\rangle = \int_{-\infty}^{+\infty} J(x,t)dx. \tag{31}$$

Note that here the spatial average is assumed, and $\langle \dot{x}(t)\rangle$ can depend on t. For the case of $g(x) = 1$, that is, if the step size in our random walk is state independent, we have

$$\mu(x) = \tanh(x), \quad V(x) = \ln[\cos(x)], \quad D = \tfrac{1}{2}. \tag{32}$$

The corresponding functions μ, D, V are shown in Fig. 2. The solution of Eqs. (27), (28), and (32) with the initial condition $P(0,x) = \delta(x - X)$, where $\delta(x - X)$ is the Dirac δ function localized at the arbitrary point X, can be found analytically [23]:

$$P(t,x) = \frac{1}{\sqrt{2\pi t}} \frac{\cosh x}{\cosh X} \exp\left(-\frac{t^2 + (x-X)^2}{2t}\right). \tag{33}$$

B. Asymptotic FP equation

To make a semianalytic approach described in [28] working (as described in the next section) we have to find the conditions where, assuming $g = \text{const}$ in Eq. (32), we have also

$\mu = \text{const}$. In our equations this is generally not the case because of the $\tanh(x)$ factor. However, as one can see from Fig. 2 and from Eq. (32), the deviation from this condition decreases exponentially with $|x|$ because $|\tanh(x)|$ exponentially fast approaches 1. Also, as one can see from Eq. (33), if we take the initial starting point X far away from the origin $X = 0$, $P(t,x)$ behaves very much like a normal Gaussian distribution which shifts with time with the constant unit speed away from $x = X$, and expands with the variance $\sigma^2 = t$.

This allows us to consider the asymptotic behavior, as the initial point X and thus x are far enough from the origin $x = 0$. We thus introduce "shifted" coordinates $x_{\leftarrow}$, $x_{\mapsto}$ as (see also Fig. 2)

$$x_{\leftarrow} = x + X, \tag{34}$$

$$x_{\mapsto} = x - X, \tag{35}$$

where $X \gg 0$ is a large arbitrary number. We will call them "asymptotic coordinates". For such defined variables, neglecting the terms which are exponentially small with $|X|$ we have from Eq. (29)

$$\mu(x_{\leftarrow},t) = -g(x_{\leftarrow},t)^2, \quad \mu(x_{\mapsto},t) = g(x_{\mapsto},t)^2, \tag{36}$$

$$D(x_{\leftarrow},t) = g(x_{\leftarrow},t)^2/2, \quad D(x_{\mapsto},t) = g(x_{\mapsto},t)^2/2, \tag{37}$$

that is, the factor $\tanh(x)$, which was present in the diffusion coefficient in Eq. (32), disappears. In the following, we will consider only the case when $x \to -\infty$, and, correspondingly, we restrict ourselves to the variable $x_{\leftarrow}$ (cf. Fig. 2). The dynamics for the case of $x \to +\infty$ is obviously analogous, only the overall drift direction will be the opposite as Eq. (36) indicates. The asymptotic FP equation for this case coincides with the original one, Eqs. (27) and (28), only written for the asymptotic coordinate $x \to x_{\leftarrow}$:

$$\partial_t P(t,x_{\leftarrow}) = -\partial_x J(t,x_{\leftarrow}), \tag{38}$$

$$J(x_{\leftarrow},y) = \mu(t,x_{\leftarrow})P(t,x_{\leftarrow}) - \partial_{x_{\leftarrow}}(D(t,x_{\leftarrow})P(t,x_{\leftarrow})). \tag{39}$$

C. FP equation for periodically varying potential

In this section we focus on the case when $g(x_{\leftarrow},t)$ changes in space and time periodically. We assume g to have period L in space $x_{\leftarrow}$. In our new asymptotic coordinates, reformulation of the FP equations (39)–(39) allows us to take advantage of such periodicity [28]. Namely, we define the reduced quantities:

$$\tilde{P}(x_{\leftarrow},t) = \sum_{j=-\infty}^{+\infty} P(x_{\leftarrow} + jL,t), \tag{40}$$

$$\tilde{J}(x_{\leftarrow},t) = \sum_{j=-\infty}^{+\infty} J(x_{\leftarrow} + jL,t). \tag{41}$$

Obviously, $\tilde{P}(x_{\leftarrow},t)$ and $\tilde{J}(x_{\leftarrow},t)$ are finite and defined in the range $x_{\leftarrow} \in [-L/2, L/2]$. Moreover, from Eqs. (40) and (41) one can see that $\tilde{P}$, $\tilde{J}$ are periodic in $x_{\leftarrow}$:

$$\tilde{P}(x_{\leftarrow},t) = \tilde{P}(x_{\leftarrow} + L,t), \quad \tilde{J}(x_{\leftarrow},t) = \tilde{J}(x_{\leftarrow} + L,t). \tag{42}$$

In the asymptotic variables $\{x_{\leftarrow},t\}$, as it follows from Eqs. (36) and (37), $\mu(x_{\leftarrow},t)$ and $D(x_{\leftarrow},t)$ are periodic in space with the same period L. Under these circumstances the FP equation written for $\tilde{P}$, $\tilde{J}$ remains the same as for P, J. That is, we have

$$\partial_t \tilde{P}(t,x_{\leftarrow}) = -\partial_{x_{\leftarrow}} \tilde{J}(t,x_{\leftarrow}), \tag{43}$$

$$\tilde{J}(x_{\leftarrow},t) = \mu(t,x_{\leftarrow})\tilde{P}(t,x_{\leftarrow}) - \partial_{x_{\leftarrow}}(D(t,x_{\leftarrow})\tilde{P}(t,x_{\leftarrow})), \tag{44}$$

where the coefficients remain the same as before, that is, are given by Eqs. (36) and (37). The advantage of such reformulation is that now we can consider only the finite interval in $x_{\leftarrow}$ from, say, $-L/2$ to $L/2$. The equation for the average drift velocity Eq. (31) also retains its form:

$$\langle \dot{x}_{\leftarrow}(t) \rangle = \int_{-L/2}^{L/2} \tilde{J}(x_{\leftarrow},t)dx. \tag{45}$$

Remarkably, the direct definition of $\langle \dot{x}_{\leftarrow}(t) \rangle$ as the average of $\dot{x}_{\leftarrow}$ with the probability distribution $\tilde{P}(x_{\leftarrow},t)$ is not valid anymore.

As an illustration of the dynamics appearing in the reduced equations, we show in Fig. 3 the dynamics of $\tilde{P}(x_{\leftarrow},t)$, $\tilde{J}(x_{\leftarrow},t)$ for the case of $g(x_{\leftarrow},t) = \text{const} = 1$ obtained using direct numerical simulations of Eqs. (43) and (44) with the initial condition $P(x_{\leftarrow},t) \propto \exp(-x_{\leftarrow}^2/0.1)$ and periodic boundary conditions. The figure shows rather rapid homogenization of $\tilde{P}(x_{\leftarrow},t)$, $\tilde{J}(x_{\leftarrow},t)$ in space because of the action of diffusion. This homogenization illustrates an important peculiarity of the reduced quantities: although the initial variables J, P have no

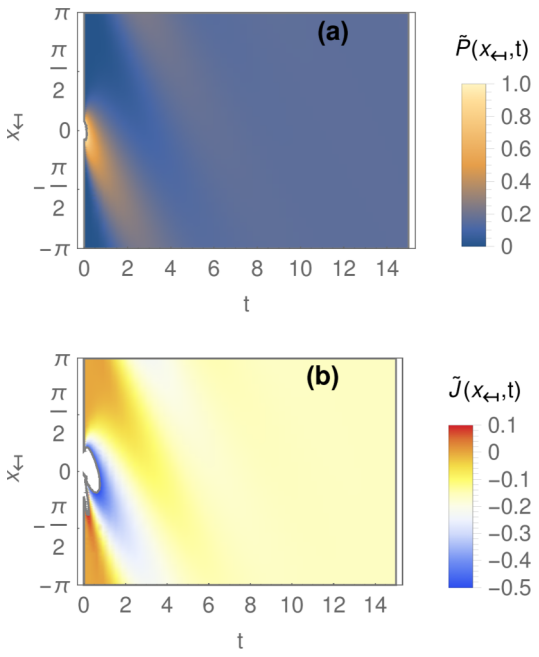

FIG. 3. The dynamics of the reduced asymptotic probability density $\tilde{P}(t,x_{\leftarrow})$ (a) and the current density $\tilde{J}(t,x_{\leftarrow})$ (b) for $g(t,x_{\leftarrow}) = 1$ obtained by direct simulations of Eqs. (40) and (41), assuming periodic boundary conditions and initial conditions described in text. In contrast to the variables P, J, the FP equation in reduced variable $\tilde{P}$, $\tilde{J}$ do have a steady state, which is in this case a homogeneous distribution.

steady state in their dynamics, the reduced quantities $\tilde{J}$, $\tilde{P}$ do have a steady state. In the case of Fig. 3 it is simply a constant which does not depend either on t or on $x_{\leftarrow\!\shortmid}$.

IV. BROWNIAN RATCHETS

One of the most interesting phenomena in Brownian flows is a possibility of so-called stochastic ratchets [27,28]. Namely, by manipulating dynamically the potential $V(x,t)$ in a Brownian flow, one can have nonzero average motion $\langle \dot{x} \rangle \neq 0$ even if the average force $\langle \mu \rangle \equiv \int \mu(x,t)dx$ is exactly zero (for every t). Here, to simplify notations, we used the denotation $\langle \dot{x} \rangle$ for the time- and space average defined as

$$\langle \dot{x} \rangle \equiv \langle \bar{\dot{x}}(\infty) \rangle, \tag{46}$$

where

$$\langle \bar{\dot{x}}(t) \rangle \equiv \frac{1}{t} \int_0^t \langle \dot{x}(\tau) \rangle \, d\tau \tag{47}$$

is the "moving average" in time of the space average. Alternatively, one can speak about a ratchet effect if a nonzero initial force $\mu \neq 0$ can be canceled or even reversed by introducing some periodic modulations of the potential. Both of these definitions are visualized in Fig. 4.

In our case it is quite clear that the average flow defined by $\mu = -1$ (in the asymptotic case $x \to x_{\leftarrow\!\shortmid}$) cannot be reversed. Otherwise, one would have a possibility to violate the conservation law of $\langle \Pi \rangle$ given by Eq. (19) by tuning, for every particular trajectory, the potential in such a way that the current system state is forced to move in the direction opposite to μ and thus bring our system to any of the states $|0\rangle$, $|1\rangle$, which would obviously violate Eq. (19).

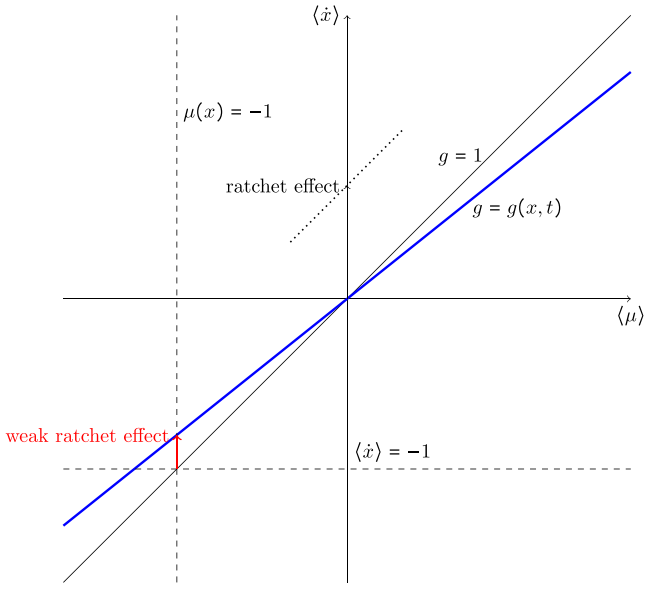

FIG. 4. Schematic representation of the Brownian ratchet effect. Without a ratchet effect ($g = 1$), a constant drift force μ leads to a net movement $\langle \dot{x} \rangle = \mu$ (black thin line). In contrast, when g changes in space and/or time (but still $\langle g \rangle = 1$), $\langle \dot{x} \rangle$ can be modified even though the average force $\langle \mu \rangle$ remains the same (blue solid and black dotted lines). Although in many other systems the Brownian ratchet effect can change the average direction of motion (see black dotted line), it is not possible in the present case—the type of ratchet which we call "weak ratchet." In this latter case, $\langle \dot{x} \rangle$ can be modified but its sign is not reversed (see blue line). The asymptotic values of μ and $\langle \dot{x} \rangle$ for $x \to -\infty$ (that is, assuming asymptotic coordinates $x_{\leftarrow\!\shortmid}$) are marked by dashed lines. Weak ratchet effect in the asymptotic case is marked by a red arrow.

Nevertheless, one can try to find a Brownian ratchet effect in a weak sense, that is, to find such a function $g(x_{\leftarrow\!\shortmid},t)$ that the the asymptotic value of $\langle \dot{x}_{\leftarrow\!\shortmid} \rangle > -1$, despite $\langle \mu \rangle = -1$. The notion of a weak ratchet effect, in comparison to a "normal" stochastic ratchet, is visualized in Fig. 4 (blue line). Weak ratchets are in close correspondence to the weak Parrondo games, where the combination of lossy games leads to a less lossy one, but still not to a winning one [30]. Of course, one can always obtain zero movement velocity by simply putting $g = 0$, that is, by reducing step size of the random walk to zero. Here we want however to investigate the effects which are independent on such raw step size reduction. To ensure this we will always normalize g so that

$$\langle g(t)^2 \rangle = 1, \tag{48}$$

where we define $\langle g(x_{\leftarrow\!\shortmid},t)^2 \rangle$ as

$$\langle g(t)^2 \rangle \equiv \frac{1}{L} \int_{-L/2}^{L/2} g(x_{\leftarrow\!\shortmid},t)^2 dx_{\leftarrow\!\shortmid}. \tag{49}$$

This condition excludes the possibility to reduce $\langle \dot{x}_{\leftarrow\!\shortmid} \rangle$ by reducing the measurement strength globally. That is, if one reduces the measurement strength near some point, one has to increase it in the vicinity of some other one.

We will now try to construct a periodic in time and space function g which allows us to reduce $|\langle \dot{x}_{\leftarrow\!\shortmid} \rangle|$, making it as small as possible.

We remark that several various types of stochastic ratchets have been considered in the literature (see [28,29] and references therein); their classification is based on the functional form of D and μ. In many commonly studied hydrodynamic Brownian flows μ and D can be varied quite independently—in contrast to our situation where independent variation of D and μ is impossible because of the common factor g. Our situation closely resembles hydrodynamic Brownian ratchets with varying friction [28,46–48]. The most studied class of ratchets is so-called pulsating ones, where μ may vary in space and time, whereas D is a constant. On the other hand, the situations when both μ and D vary in space or, alternatively, in time, were also considered under the names Seebeck or temperature ratchets, correspondingly. They can be mapped, by suitable change of variable, to the pulsating ratchets.

In our case, as one can see, the situation when g is changing in time but not in space provides no possibility for any ratchet effect. Namely, in this case Eq. (45) can be calculated directly by integrating Eq. (44) with the boundary conditions Eq. (42), giving $\langle \dot{x}_{\leftarrow\!\shortmid}(t) \rangle = -1$. We have then $\tilde{P} \to \text{const} = 1/L$, that is, full homogenization of $\tilde{P}$ will take place, exactly as in the case of $g = 1$.

We can therefore consider the cases when μ and D change both in time and space or only in space. For the presence of the ratchet effect, the symmetry of the μ and D are of critical importance. In general, "almost all" functions except the ones processing certain particular symmetry properties allow the

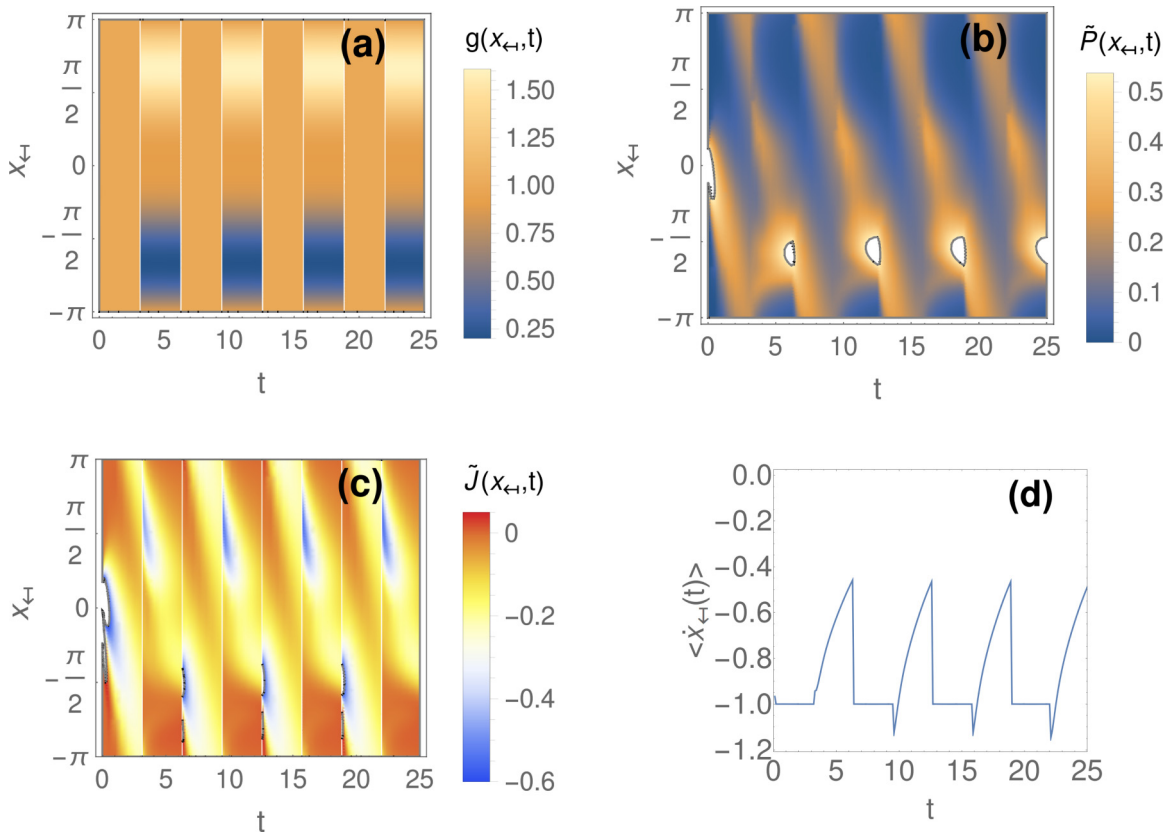

FIG. 5. Brownian ratchet effect for $g(x_{\leftrightarrow},t)$ varying in space and time. (a) $g(x_{\leftrightarrow},t)$, as given by Eqs. (50)–(53). (b),(c) Reduced asymptotic probability density $\tilde{P}(x_{\leftrightarrow})$ and the current density $\tilde{J}(x_{\leftrightarrow})$ obtained by direct simulations of Eqs. (43) and (44) with periodic boundary conditions and initial conditions as in Fig. 3. (d) Averaged current $\langle \dot{x}_{\leftrightarrow}(t)\rangle$ in dependence on time.

ratchet effect [28,29]. Nevertheless, no analytical symmetry relation is known, to our knowledge, for the case when both μ and D are arbitrary functions of space and time. For the case when μ and D are only space dependent, the situation is simpler and is discussed in the next section.

One of the most well-known types of ratchets is an on-off tilting ratchet, were the diffusion D is constant and the asymmetric potential V is switched on and off. At the on stage, the particle moves to the minimum of the potential and therefore becomes well localized. When the potential is switched off, diffusion leads to a broadening of the particle's wave packet. Switching the potential on again makes the particle feel the force. If the potential is asymmetric, the force is also asymmetric, leading to an average current.

Having in mind the above, we first probe functions $g(x_{\leftrightarrow},t)$ which have the following exemplary form:

$$g(x_{\leftrightarrow},t) = C(t)\{1 + F(x_{\leftrightarrow})f(t)\}, \tag{50}$$

where the function $f(t)$ is periodic in time which models the switch-on and -off behavior, and $F(x)$ is periodic in space, but might be asymmetric. The normalizing factor $C(t)$ is obtained from Eq. (48). To start with, we will try the following functions:

$$f(t) = \{\mathrm{sgn}[\sin(t)] - 1\}/2, \tag{51}$$

$$F(x_{\leftrightarrow}) = a[\sin(x_{\leftrightarrow}) + b\sin(2x_{\leftrightarrow})], \tag{52}$$

$$a = -0.6, \quad b = -0.5. \tag{53}$$

Here, $f(t)$ works as a switcher which is active only half of the period, a determines the "amplitude" of the periodic potential, whereas b is selected here in such a way that the shape of g resembles a "sawtooth" one, in order to introduce some spatial asymmetry into the profile g. Indeed, this shape of F is simply the decomposition of the ideal sawtooth shape $F_s(x) = \sum_{n=1}^{\infty}(-1)^n \sin nx/n$ which is cut after the second term.

The resulting dynamics are plotted in Fig. 5. Namely, the shape of g is presented in Fig. 5(a) whereas Fig. 5(b) and Fig. 5(c) show the temporally and spatially resolved probability and current. To calculate Fig. 5, the boundary and initial conditions were taken as in Fig. 3. One can see from Fig. 5(b) that when the space-varying potential is on, the probability density $\tilde{P}$ concentrates in the regions where g (and thus D, μ) is minimal. When it is off, the wave packet starts to diverge (and at the same time is moving to the negative direction of $x_{\leftrightarrow}$). This behavior is thus different from typical pulsating ratchets in the sense that when the potential is switched on, the particle is localized in the minima of g (and thus in the minima of D and μ, and not of the potential as it happens in pulsating ratchets). In Fig. 5(d) one can see that the current $\langle \dot{x}_{\leftrightarrow}(t)\rangle$ approaches, after a short transition process, a stationary regime of oscillations in time with a period 2π. The long time behavior of $\langle \bar{\dot{x}}_{\leftrightarrow}(t)\rangle$ [Eq. (47)] is shown in Fig. 6, where it is seen that this average approaches ≈ -0.86 instead of -1 as in the case of constant $g = 1$, $\mu = -1$, thus clearly showing the ratchet effect.

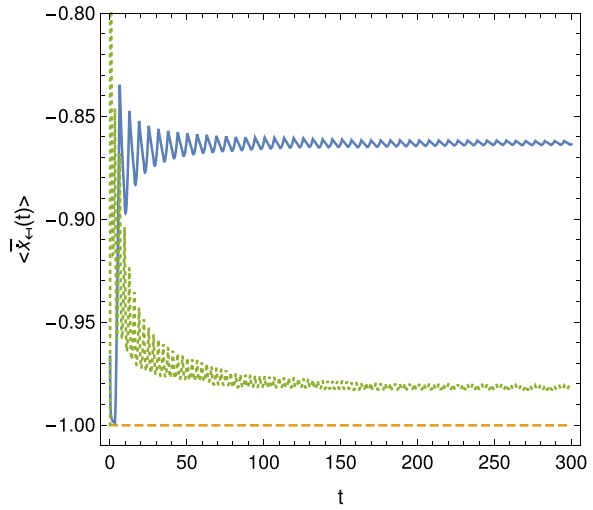

FIG. 6. Dependence of the moving temporal average $\langle \bar{\dot{x}}_{\leftarrow} \rangle$ given by Eq. (47) on the averaging time interval t. In the case of constant $g = 1$ (orange dashed line) this quantity quickly approaches -1 (no ratchet effect), whereas in the case of varying measurement strength with the parameters Eqs. (50)–(53) (blue solid line) it approaches ≈ -0.86, demonstrating a weak Brownian ratchet. The effect strength depends on the function shape. For instance, the green dotted line shows the case Eq. (50) with the spatial dependence $F(x)$ given by Eq. (52) with $a = -0.8$, $b = 0$, and $f(t) = \mathrm{sgn} \sin t$.

To check the stability of the effect, simulations were made for different functions $f(t)$, $F(x)$. For instance, in Fig. 6 the case with $b = 0$ and $f(t) = \mathrm{sgn}[\sin(t)]$ is also plotted. In this case, the ratchet effect is definitely smaller but still persists. As said, the condition Eq. (48) excludes the effect of bare step size reduction in this random walk, demonstrating that the ratchet effect is a dynamical phenomenon independent from the step size.

V. SEEBECK RATCHETS AND DYNAMICAL LOCALIZATION

In general, the ratchet effect can appear if D, μ change only in space. In this case, one may have the diffusion D and the potential V defined by Eq. (30) being not in phase [28], which in our case is typically fulfilled, since $D \sim \mu$, $\mu = -\partial_x V$ (that is, if $D \sim \sin x$, then $V \sim \cos x$; see also Fig. 8). Such ratchets are typically known as Seebeck ones [28]. For Seebeck ratchets, an analytical condition exists which determines the absence of the ratchet effect. In particular, if we consider the case with no average force ($\langle \mu \rangle = 0$) and if $\int_{-L/2}^{L/2} \mu(x)/D(x) dx = 0$, no ratchet effect is present [49,50]. In our case, $\langle \mu \rangle \neq 0$ so that the condition above cannot be applied directly. Nevertheless, we can, using the replacement $x_{\leftarrow} \to x_{\leftarrow}$, $t \to t - x_{\leftarrow}$, reduce our equation to the case with $\langle \mu \rangle = 0$. In this case we have $\langle \dot{x}_{\leftarrow} \rangle \to \langle \dot{x}_{\leftarrow} \rangle + 1$. Afterwards, we can apply the above formula, which gives us the criterion for the absence of the ratchet effect for our case in the form

$$\frac{1}{L} \int_{-L/2}^{L/2} \frac{1}{g^2(x_{\leftarrow})} dx_{\leftarrow} = 1. \tag{54}$$

That is, for a typical function g [which satisfies Eq. (48)] we should expect the presence of a ratchet effect, unless Eq. (54) is also valid. An exemplary profile of g which we use to test the Seebeck ratchet numerically is given by Eq. (50) with $f(t) = 1$ and $F(x_{\leftarrow})$ defined by Eq. (52) with

$$a = -0.8, \quad b = 0, \tag{55}$$

and is shown in Fig. 7(a). For such a function g, as one can see in Fig. 7(b), the average current $\langle \dot{x}_{\leftarrow} \rangle$ can be also larger than -1; in the case of Fig. 7 it approaches ≈ -0.2 as one can see in Fig. 7(d). In this case, the initial distribution is quickly rearranged to a stationary (but inhomogeneous) one.

Now, again, the system is located mostly near the minimum of g. This allows interpretation of the Seebeck ratchet effect in the present case in the terms of a "dynamical localization". Namely, let us observe the potential $V(x_{\leftarrow})$ as shown in Fig. 8 (solid blue line). One can see that $V(x_{\leftarrow})$ approaches a flat region (where it is almost constant) close to $x_{\leftarrow} = \pi/2$. That is, there is almost no effective force at that point. If our effective "particle" approaches this region, it nearly stops. Nevertheless, the particle experiences some small drift to the negative direction of $x_{\leftarrow}$.

Going one step further, we consider now the case when $g = 0$ at some point. In this case we also expect localization shown in the previous example. But more interesting dynamics will also appear as we will see below. In general, to observe localization, it is not necessary to take the periodic potential as it was in the previous example. We now consider the global dynamics related to localization, and therefore we return back from "asymptotic coordinate" $x_{\leftarrow}$ to the initial coordinate x and thus to the FP equation as written in Eqs. (27) and (28). We assume also for simplicity that $g(x)$ approaches zero only in one single point X, that is, $g \to 0$ as $x \to X$. Returning to our initial qubit, the state $|X\rangle$ is given by

$$|X\rangle = A|0\rangle + B|1\rangle; \tag{56}$$

$$A = \sqrt{\Pi(X)}, \quad B = \sqrt{1 - \Pi(X)}, \tag{57}$$

where $\Pi(X)$ is given by Eq. (11). As we will see later the trajectory cannot cross $|X\rangle$ in this case. A state $|x\rangle$ located between of $|0\rangle$ and $|X\rangle$ will approach either $|0\rangle$ or $|X\rangle$ as $t \to \infty$. Analogously, a state located initially between $|X\rangle$ and $|1\rangle$ will approach either $|X\rangle$ or $|1\rangle$ [see Fig. 9(b)]. We note a similarity to the initial system with the state-independent coupling strength $g = 1$ in this limiting dynamics [where the limiting states are $|0\rangle$ and $|1\rangle$, see Fig. 9(a)]. One can make this analogy exact by considering the FP equation in coordinates $\Pi(x)$ defined in Eq. (11) which is given by (see also Appendix D)

$$\partial_t P(t, \Pi) = \partial_{\Pi\Pi}(D(\Pi) P(t, \Pi)) \tag{58}$$

$$D(\Pi) = 2(\Pi - 1)^2 \Pi^2 g^2(\Pi), \tag{59}$$

so that the diffusion coefficient $\mu = 0$ in these coordinates. We remark that for $|0\rangle$ and $|1\rangle$ ($\Pi = 0$ and $\Pi = 1$ correspondingly) $D(\Pi) = 0$.

Let us make the denotation $\Pi(X) \equiv \Pi_X$; we have thus $g(\Pi_X) = 0$. We also consider only one case when the initial state is in between $|0\rangle$ and $|X\rangle$, that is, $x(t = 0) < X$ and

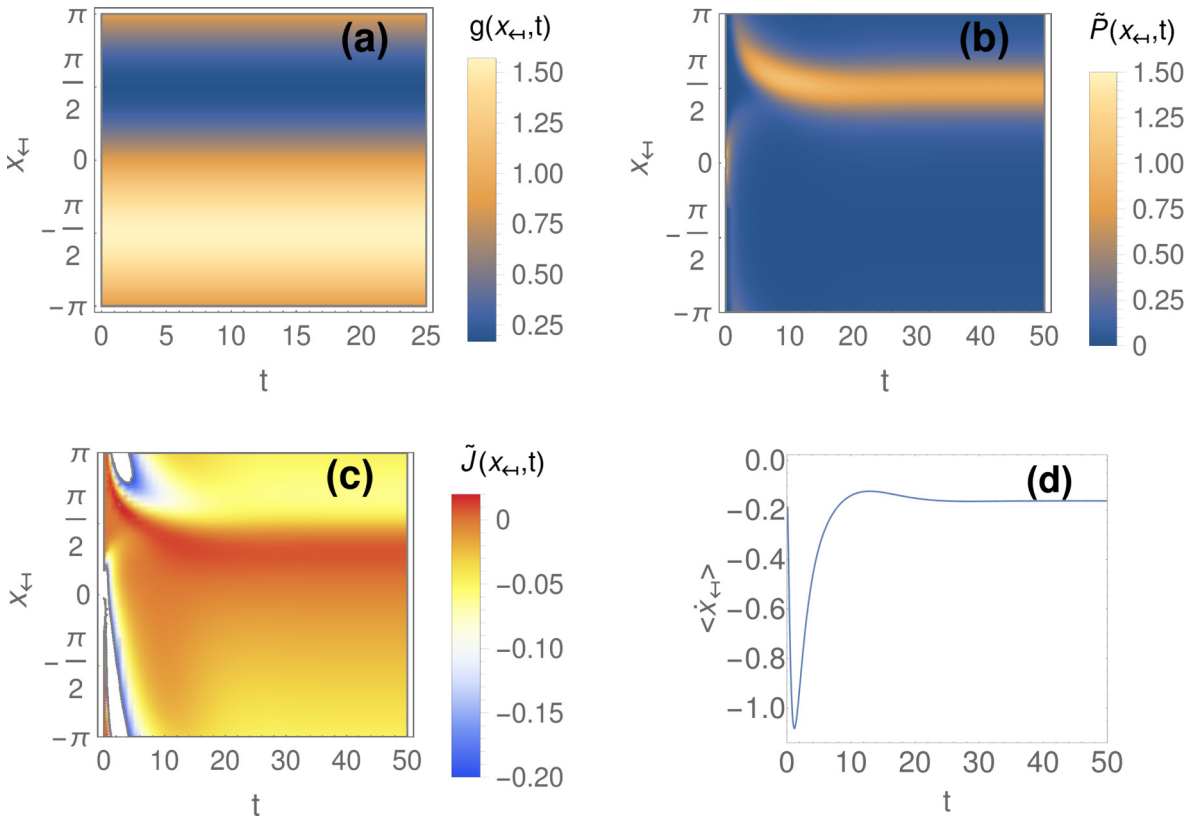

FIG. 7. Seebeck ratchet and dynamical localization effect for $g(x_{\leftarrow\!|})$ dependent only on spatial coordinate. (a) $g(x_{\leftarrow\!|},t)$ given by Eq. (50) with $C(t) = \text{const}$, $f(t) = 1$, and other parameters defined by Eqs. (52) and (55). (b),(c) Reduced asymptotic probability density $\tilde{P}(x_{\leftarrow\!|})$ and the current density $\tilde{J}(x_{\leftarrow\!|})$ obtained by direct simulations of Eqs. (43) and (44) with periodic boundary conditions and initial conditions as in Fig. 3. (d) Spatially averaged current $\langle \dot{x}_{\leftarrow\!|} \rangle$ in dependence on time.

$\Pi(t=0) < \Pi_X$ [see Fig. 9(b), red lines]. In this case we can obviously define such a function $\tilde{g}(\Pi)$ that

$$g(\Pi) = \frac{\Pi_X - \Pi}{1 - \Pi}\tilde{g}(\Pi), \tag{60}$$

which is possible without singularities since $1 - \Pi > 1 - \Pi_X > 0$. Here, $\tilde{g} \geqslant 0$ does not anymore necessarily approach zero as $\Pi \to \Pi_X$. Now, by making a variable change

$$\tilde{\Pi} = \Pi/\Pi_X, \quad \tilde{t} = \Pi_X^2 t, \tag{61}$$

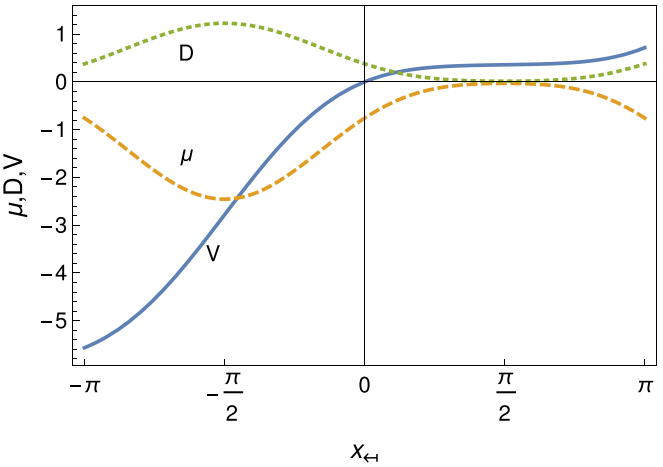

FIG. 8. Diffusion $D(x)$ (solid blue line), shift $\mu(x)$ (dashed red line), and the effective potential $V(x)$ (dotted yellow line, normalized to a constant $c = 0.1$ for better visibility) in dependence on $x_{\leftarrow\!|}$ with $g(x_{\leftarrow\!|})$ being time independent, that is, given by Eq. (50) with $C(t) = \text{const}$, $f(t) = 1$, and other parameters defined by Eqs. (52) and (55).

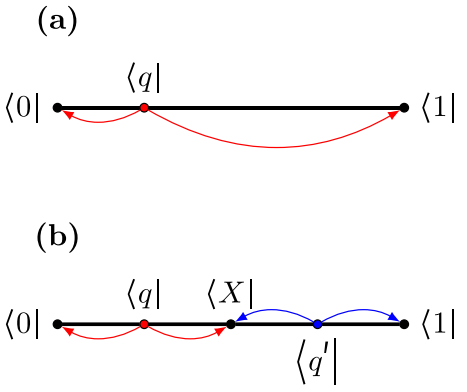

FIG. 9. The limits $t \to \infty$ of the weak measurement sequence in the case of $g = 1$ (a) and in the case of $g(x,t)$ such that $g(x) \to 0$ as $x \to X$ (b); the coordinate X corresponds to the qubit state $|X\rangle$. In the former case, an arbitrary state $|q\rangle$ approaches either to $|0\rangle$ or $|1\rangle$, whereas in case (b) the state may also have $|X\rangle$ as a limiting point. Some states (such as $|q\rangle$) tend to either $|0\rangle$ or $|X\rangle$, the others (as $|q'\rangle$) approach $|1\rangle$ or $|X\rangle$.

we arrive at a new FP equation:

$$\partial_{\tilde{t}} P(\tilde{t},\tilde{\Pi}) = \partial_{\tilde{\Pi}\tilde{\Pi}}(\tilde{D}(\tilde{\Pi})P(\tilde{t},\tilde{\Pi})), \tag{62}$$

$$\tilde{D}(\tilde{\Pi}) = 2(\tilde{\Pi}-1)^2\tilde{\Pi}^2\tilde{g}^2(\tilde{\Pi}), \tag{63}$$

where $\tilde{g}(\tilde{\Pi}) = \tilde{g}(\Pi\Pi_X)$. One can see that Eqs. (58) and (59) and Eqs. (62) and (63) are completely equivalent. That is, the dynamics of the random walk between $|0\rangle$ and $|X\rangle$ and between $|0\rangle$ and $|1\rangle$ can be one to one mapped to each other. In particular, the dynamics of the random walk with $\tilde{g}=1$, that is, with $g(\Pi) = (\Pi_X - \Pi)/(1-\Pi)$, is completely equivalent to the dynamics of the simplest random walk with $g=1$. The system with $\tilde{g}=1$ behaves near $|X\rangle$ in the same way as the system with $g=1$ near the state $|1\rangle$, for instance, the time of arrival to the point $|X\rangle$ is infinite. This is obviously true for any other bounded functions $\tilde{g}$ obeying Eq. (48) and such that $g>0$.

This allows us also to calculate straightforwardly the probability of the outcomes $|0\rangle$ or $|X\rangle$ (respectively $|X\rangle$ or $|1\rangle$) as $t\to\infty$. In our initial system with $g=1$ the *a priori* probabilities to have $|0\rangle$ or $|1\rangle$ would be given by $\Pi(x)$ and $1-\Pi(x)$, correspondingly, and, according to Eq. (19), also do not depend on the measurement strength $g(x,t)$ (unless g approaches zero somewhere). By rescaling the latter situation using Eq. (61) we see that starting from the state $|x\rangle$ we reach $|0\rangle$ or $|X\rangle$ (respectively $|X\rangle$ and $|1\rangle$) with the probabilities $\tilde{\Pi}(x) = \Pi(x)/\Pi_X$ and $1-\tilde{\Pi}(x) = 1-\Pi(x)/\Pi_X$. These probabilities also do not depend on the measurement strength (unless it approaches zero somewhere else at $x<X$). In the same way, if $|x\rangle$ is in between $|X\rangle$ and $|1\rangle$, we obtain that the probabilities to reach $|X\rangle$ or $|1\rangle$ are $[\Pi(x)-\Pi_X]/(1-\Pi_X)$ and $[1-\Pi(x)]/(1-\Pi_X)$ respectively.

VI. CONCLUSIONS

In the present article we have considered quantum trajectories resulting from a sequence of weak measurements, in the simplest one-dimensional settings, but assuming the measurement strength depending on the step number n and on the current state of the system described by the coordinate x on the line. Of course, the current state cannot be inferred from the measurement directly, in contrast to classical systems. Nevertheless, if the initial state and the parameters of the weak measurements are known, all the subsequent positions of the system can be inferred from the sequence of the measurement outcomes, and thus the conditional measurement strength can be well defined.

Such measurement process, in the limit of infinitely small steps, leads to a diffusive dynamics with both drift and diffusion depending on the coordinate x and time t. In fact, the dynamics arising in such a case is quite similar to, for instance, an overdamped Brownian particle in a flow with a varying friction coefficient. In this article we discussed the nontrivial dynamics arising due to this analogy.

For instance, an exciting phenomenon arising in Brownian flows is the stochastic ratchet effect, which allows us to "rectify" Brownian motion using periodically varying potential. Such potential does not introduce any net force by itself, nevertheless allowing to push particles in the direction opposite to the flow. As it has been shown here, in our case we can achieve only a weak form of the stochastic ratchet effect. That is, we cannot reverse the overall drift direction of the quantum trajectories, but only slow down this motion. The ratchet effect manifests itself in the localization of the particle in the areas where the measurement strength is reduced and thus the effective force is minimal.

Finally, we considered the case when the step size approaches zero as the system approaches some state $|X\rangle$. No quantum trajectory can cross the singularity point arising in this case. Moreover, the trajectories approach such singularity in the infinite time in a similar way as they approach the "normal" basis states. The FP equation demonstrates remarkable self-similarity in this case: the arbitrary quantum walk between any subsequent zeros can be mapped to a quantum walk between $|0\rangle$ and $|1\rangle$ with the nonvanishing measurement strength.

The effects predicted here can be tested in the measurement-only quantum control settings, such as, for instance, the one recently realized experimentally using defect-in-diamond-based qubits [2], but also in other setups where weak quantum measurements or control, based on weak measurements, were realized, for instance for photon-based [25], ultracold-atom-based [1,9], or superconducting-based [3] qubits.

ACKNOWLEDGMENTS

The author is thankful to Niedersächsisches Vorab, Project No. ZN3061, and to the Deutsche Forschungsgemeinschaft (DFG), Project No. BA 4156/4-1, for financial support.

APPENDIX A: DERIVATION OF THE EXPRESSION FOR STEP SIZE

To derive the step size $\epsilon_i(x_n) \equiv x_{n+1} - x_n$ on the nth step of our random walk, we use Eqs. (3)–(7) and the relation

$$\sin^2\theta_n = \frac{1+\tanh x_n}{2}. \tag{A1}$$

For instance, in the case when the measurement of the ancilla $|a\rangle$ gives $|0\rangle$, we have from Eqs. (3)–(7)

$$\sin\theta_{n+1} = \sin\theta_n \cos(\delta+\alpha)/\sqrt{p_0}, \tag{A2}$$

and thus, using Eq. (A1):

$$\frac{1+\tanh x_{n+1}}{2} = \frac{(1+\tanh x_n)\cos^2(\delta+\alpha)}{2p_0}. \tag{A3}$$

Hence, the expression for $\epsilon_0(x)$ (redefining x_n as x since x_n is arbitrary) is

$$\epsilon_0(x) = \operatorname{atanh}\left(\frac{(1+\tanh x)\cos^2(\delta+\alpha)}{p_0(x)} - 1\right) - x. \tag{A4}$$

In the same way, if $|a\rangle$ collapses to $|1\rangle$ upon the measurement, we have

$$\sin\theta_{n+1} = \sin\theta_n \sin(\delta+\alpha)/\sqrt{p_1}, \tag{A5}$$

and thus we obtain for $\epsilon_1(x)$

$$\epsilon_1(x) = \operatorname{atanh}\left(\frac{(1+\tanh x)\sin^2(\delta+\alpha)}{p_1(x)} - 1\right) - x. \tag{A6}$$

Now we can calculate analytically the expression for $d\epsilon_i(x)/dx$, which, after some algebraic transformations, can be shown to be zero. Thus, $\epsilon_i(x) = \epsilon_i(0) \equiv \epsilon_i$ and we can take

$x = 0$ in Eqs. (4) and (6), thus obtaining expressions (14) and (15).

APPENDIX B: QUANTUM TRAJECTORIES WITH CONSTANT MEASUREMENT PARAMETERS

In the case of a constant x-independent step (and only in this case) it is constructive to analyze ϵ_i, p_i on a more general level by introducing the "average step" $\mu(x)$:

$$\mu(x)=\mu_0(x)+\mu_1(x), \quad \mu_i(x)=\epsilon_i p_i(x), \quad i=0,1. \tag{B1}$$

μ defines an "average direction" of evolution: towards $+\infty$ or $-\infty$.

Equations (B1) are simplified when δ is small (assuming fixed $\alpha > 0$), so we can decompose Eqs. (12)–(15) in series in δ. In this case, up to the second order of δ we have

$$\mu(x) = \delta^2 \tanh(x) + O(\delta^3), \tag{B2}$$

$$2\mu_0(x)=\delta \sin(2\alpha)+\delta^2[4\Pi(x)\sin^2\alpha-1]+O(\delta^3), \tag{B3}$$

$$2\mu_1(x) = -\delta \sin(2\alpha) + \delta^2[4\Pi(x)\cos^2\alpha - 1] + O(\delta^3), \tag{B4}$$

where $\Pi(x)$ is given by Eq. (11). Since $\operatorname{sgn} x = \operatorname{sgn}\tanh x$ Eq. (B2) demonstrates a "weak attraction" of the dynamics to the nearest state as shown in Fig. 2. We also can define in this case a quantity D, which has the meaning of a diffusion coefficient:

$$D(x) = \frac{1}{2}\sum_i p_i(x)\epsilon_i^2. \tag{B5}$$

It is easy to see that in the limit of small δ (assuming $\alpha = \text{const}$) we have

$$D(x) = \tfrac{1}{2}\delta^2 + O(\delta^3). \tag{B6}$$

APPENDIX C: DERIVATION OF THE FOKKER-PLANCK EQUATION

We derive the FP equation using the standard integral approach [42]. Namely, we consider an arbitrary function $h(x)$ which has a finite support, that is, localized inside the integration area and is zero together with all of its derivatives for large enough $|x|$. We also assume that it is smooth enough. Then, we write the expression for $\int h(x)\partial_t P(t,x)dx$, assuming integration over the whole real axis:

$$\tau_n \int h(x)\partial_t P(t,x)dx \approxeq \int h(x)[P(t+\tau,x) - P(t,x)]dx, \tag{C1}$$

Expressing $P(t+\tau_n,x)$ through $P(t,x)$ using Eq. (17) and assuming $t = \sum_n \tau_n$, replacing variables in two integral parts as $x \to x_i(x)$ followed by redefining $x_i \to x$, and finally expanding $h(x+\epsilon) \approxeq h(x) + \epsilon h'(x) + \epsilon^2 h''(x)/2$, we transform the later expression into

$$\int P(t,x)\left(\sum_i p_i\left(h'(x)\epsilon_i(x) + h''(x)\epsilon_i^2(x)/2\right)\right)dx. \tag{C2}$$

Applying integration by parts we have finally

$$\int h(x)\{-\partial_t P(t,x) - \partial_x[\mu(x,t)P(t,x)] + \partial_{xx}[D(x,t)P(t,x)]\}dx = 0, \tag{C3}$$

where

$$\mu(x,t) = \sum_i \left.\frac{p_i(x,n)\epsilon_i(x,n)}{\tau_n}\right|_{n\to t}, \tag{C4}$$

$$D(x,t) = \sum_i \left.\frac{p_i(x,n)\epsilon_i^2(x,n)}{2\tau_n}\right|_{n\to t}. \tag{C5}$$

For small δ and α_n being constant for every n we have, up to the second order of δ,

$$\sum_i p_i(x,t)\epsilon_i(x,t) = \delta_n(x)^2 \tanh(x) + O(\delta_n(x)^3), \tag{C6}$$

$$\sum_i p_i(x,t)\epsilon_i^2(x,t) = \delta_n(x)^2 + O(\delta_n(x)^3). \tag{C7}$$

Taking into account Eq. (24), we finally arrive at Eqs. (26)–(29).

APPENDIX D: FP COEFFICIENTS μ AND D IN DIFFERENT COORDINATES

We may easily change the variables $x \to y(x)$ in the FP equation by the known rule [51]

$$\mu(y) = \mu(x)\partial_x y(x) + D(x)\partial_{xx} y(x), \tag{D1}$$

$$D(y) = D(x)[\partial_x y(x)]^2. \tag{D2}$$

In θ coordinates, given by Eq. (10), we have

$$\mu(\theta) = -\frac{g^2(\theta)\sin(4\theta)}{8}, \quad D(\theta) = \frac{g^2(\theta)\sin^2(2\theta)}{8}. \tag{D3}$$

For the coordinates $\Pi(x)$ we obtain

$$\mu(\Pi) = 0, \quad D(\Pi) = 2(\Pi-1)^2\Pi^2 g^2(\Pi). \tag{D4}$$

The last equation for $\mu(\Pi)$ reflects the conservation of $\langle\Pi\rangle$ as given by Eq. (19).

[1] Y. S. Patil, S. Chakram, and M. Vengalattore, Measurement-Induced Localization of an Ultracold Lattice Gas, Phys. Rev. Lett. **115**, 140402 (2015).

[2] M. S. Blok, C. Bonato, M. L. Markham, D. J. Twitchen, V. V. Dobrovitski, and R. Hanson, Manipulating a qubit through the backaction of sequential partial measurements and real-time feedback, Nat. Phys. **10**, 189 (2014).

[3] K. W. Murch, S. J. Weber, C. Macklin, and I. Siddiqi, Observing single quantum trajectories of a superconducting quantum bit, Nature (London) **502**, 211 (2013).

[4] M. Hatridge, S. Shankar, M. Mirrahimi, F. Schackert, K. Geerlings, T. Brecht, K. M. Sliwa, B. Abdo, L. Frunzio, S. M. Girvin, R. J. Schoelkopf, and M. H. Devoret, Quantum back-action of an individual variable-strength measurement, Science **339**, 178 (2013).

[5] H. M. Wiseman, Quantum control: Squinting at quantum systems, Nature (London) **470**, 178 (2011).

[6] S. Ashhab and F. Nori, Control-free control: Manipulating a quantum system using only a limited set of measurements, Phys. Rev. A **82**, 062103 (2010).

[7] C. Guerlin, J. Bernu, S. Deléglise, C. Sayrin, S. Gleyzes, S. Kuhr, M. Brune, J.-M. Raimond, and S. Haroche, Progressive field-state collapse and quantum non-demolition photon counting, Nature (London) **448**, 889 (2007).

[8] S. Gleyzes, S. Kuhr, Ch. Guerlin, J. Bernu, S. Deleglise, U. Busk Hoff, M. Brune, J.-M. Raimond, and S. Haroche, Quantum jumps of light recording the birth and death of a photon in a cavity, Nature (London) **446**, 297 (2007).

[9] K. W. Murch, K. L. Moore, S. Gupta, and D. M. Stamper-Kurn, Observation of quantum-measurement backaction with an ultracold atomic gas, Nat. Phys. **4**, 561 (2008).

[10] S. Gammelmark, B. Julsgaard, and K. Mølmer, Past Quantum States of a Monitored System, Phys. Rev. Lett. **111**, 160401 (2013).

[11] A. Pechen, N. Il'in, F. Shuang, and H. Rabitz, Quantum control by von neumann measurements, Phys. Rev. A **74**, 052102 (2006).

[12] G. Gordon, I. E. Mazets, and G. Kurizki, Quantum particle localization by frequent coherent monitoring, Phys. Rev. A **87**, 052141 (2013).

[13] J. B. Mackrory, K. Jacobs, and D. A. Steck, Reflection of a particle from a quantum measurement, New J. Phys. **12**, 113023 (2010).

[14] H. M. Wiseman and G. J. Milburn, *Quantum Measurement and Control* (Cambridge University Press, Cambridge, England, 2010).

[15] G. A. Paz-Silva, A. T. Rezakhani, J. M. Dominy, and D. A. Lidar, Zeno Effect for Quantum Computation and Control, Phys. Rev. Lett. **108**, 080501 (2012).

[16] C. M. Caves and G. J. Milburn, Quantum-mechanical model for continuous position measurements, Phys. Rev. A **36**, 5543 (1987).

[17] O. Oreshkov and T. A. Brun, Weak Measurements are Universal, Phys. Rev. Lett. **95**, 110409 (2005).

[18] M. Varbanov and T. A. Brun, Decomposing generalized measurements into continuous stochastic processes, Phys. Rev. A **76**, 032104 (2007).

[19] Y. Aharonov, D. Z. Albert, and L. Vaidman, How the Result of a Measurement of a Component of the Spin of a Spin-1/2 Particle can Turn Out to be 100, Phys. Rev. Lett. **60**, 1351 (1988).

[20] J. Dressel and A. N. Jordan, Weak Values are Universal in Von Neumann Measurements, Phys. Rev. Lett. **109**, 230402 (2012).

[21] J. S. Lundeen and Ch. Bamber, Procedure for Direct Measurement of General Quantum States Using Weak Measurement, Phys. Rev. Lett. **108**, 070402 (2012).

[22] V. P. Belavkin, A new wave equation for a continuous nondemolition measurement, Phys. Lett. A **140**, 355 (1989).

[23] N. Gisin, Quantum Measurements and Stochastic Processes, Phys. Rev. Lett. **52**, 1657 (1984).

[24] H. M. Wiseman, Quantum trajectories and quantum measurement theory, Quantum Semiclass. Opt. **8**, 205 (1996).

[25] G. G. Gillett, R. B. Dalton, B. P. Lanyon, M. P. Almeida, M. Barbieri, G. J. Pryde, J. L. O'Brien, K. J. Resch, S. D. Bartlett, and A. G. White, Experimental Feedback Control of Quantum Systems Using Weak Measurements, Phys. Rev. Lett. **104**, 080503 (2010).

[26] R. I. Karasik and H. M. Wiseman, How Many Bits does it Take to Track an Open Quantum System? Phys. Rev. Lett. **106**, 020406 (2011).

[27] P. Hänggi and F. Marchesoni, Artificial brownian motors: Controlling transport on the nanoscale, Rev. Mod. Phys. **81**, 387 (2009).

[28] P. Reimann, Brownian motors: Noisy transport far from equilibrium, Phys. Rep. **361**, 57 (2002).

[29] O. M. Braun and Y. Kivshar, *The Frenkel-Kontorova Model: Concepts, Methods, and Applications, Physics and Astronomy Online Library* (Springer, New York, 2004).

[30] D. Wu and K. Y. Szeto, Extended Parrondo's game and Brownian ratchets: Strong and weak Parrondo effect, Phys. Rev. E **89**, 022142 (2014).

[31] M. Velez, J. I. Martin, J. E. Villegas, A. Hoffmann, E. M. González, J. L. Vicent, and I. K. Schuller, Superconducting vortex pinning with artificial magnetic nanostructures, J. Magn. Magn. Mater. **320**, 2547 (2008).

[32] C. C. de Souza Silva, J. Van de Vondel, M. Morelle, and V. V. Moshchalkov, Controlled multiple reversals of a ratchet effect, Nature (London) **440**, 651 (2006).

[33] J. E. Villegas, E. M. Gonzalez, M. P. Gonzalez, J. V. Anguita, and J. L. Vicent, Experimental ratchet effect in superconducting films with periodic arrays of asymmetric potentials, Phys. Rev. B **71**, 024519 (2005).

[34] P. G. de Alaiza Martínez, I. Babushkin, L. Bergé, S. Skupin, E. Cabrera-Granado, C. Köhler, U. Morgner, A. Husakou, and J. Herrmann, Boosting Terahertz Generation in Laser-Field Ionized Gases Using a Sawtooth Wave Shape, Phys. Rev. Lett. **114**, 183901 (2015).

[35] A. A. Klyukanov, N. A. Loiko, I. V. Babushkin, and V. Gurau, Hartree-fock semiconductor bloch equations and charge density correlations, in *XVII International Conference on Coherent and Nonlinear Optics (ICONO 2001)* (International Society for Optics and Photonics, San Francisco, CA, 2002), p. 301.

[36] J. M. R. Parrondo, How to cheat a bad mathematician, *EEC HC&M Network on Complexity and Chaos* (ISI, Torino, Italy, 1996).

[37] A. Allison and D. Abbott, The physical basis for Parrondo's games, Fluct. Noise Lett. **2**, L327 (2002).

[38] Ł. Pawela and J. Sładkowski, Cooperative quantum Parrondos games, Phys. D (Amsterdam, Neth.) **256**, 51 (2013).

[39] C. M. Chandrashekar and S. Banerjee, Parrondos game using a discrete-time quantum walk, Phys. Lett. **A375**, 1553 (2011).

[40] D. Bulger, J. Freckleton, and J. Twamley, Position-dependent and cooperative quantum Parrondo walks, New J. Phys. **10**, 093014 (2008).

[41] A. P. Flitney, J. Ng, and D. Abbott, Quantum Parrondo's games, Phys. A (Amsterdam, Neth.) **314**, 35 (2002).

[42] C. W. Gardiner and C. Gardiner, *Stochastic Methods: A Handbook for the Natural and Social Sciences* (Springer, Berlin, 2009), Vol. 4.

[43] T. A. Brun, A simple model of quantum trajectories, Am. J. Phys. **70**, 719 (2002).

[44] M. Bauer, T. Benoist, and D. Bernard, Repeated quantum nondemolition measurements: Convergence and continuous time limit, in *Annales Henri Poincaré* (Springer, New York, 2013), p. 1.

[45] Ch. R. Doering, Stochastic ratchets, Phys. A (Amsterdam, Neth.) **254**, 1 (1998).

[46] R. H. Luchsinger, Transport in nonequilibrium systems with position-dependent mobility, Phys. Rev. E **62**, 272 (2000).

[47] P. Lançon, G. Batrouni, L. Lobry, and N. Ostrowsky, Drift without flux: Brownian walker with a space-dependent diffusion coefficient, Europhys. Lett. **54**, 28 (2001).

[48] R. Krishnan, S. Singh, and G. W. Robinson, Space-dependent friction in the theory of activated rate processes, Phys. Rev. A **45**, 5408 (1992).

[49] N. G. Van Kampen, Relative stability in nonuniform temperature, IBM J. Res. Dev. **32**, 107 (1988).

[50] R. Landauer, Motion out of noisy states, J. Stat. Phys. **53**, 233 (1988).

[51] H. Risken, *The Fokker-Planck Equation: Methods of Solution and Applications* (World Scientific, Singapore, 1984).